ChemComm

Accepted Manuscript

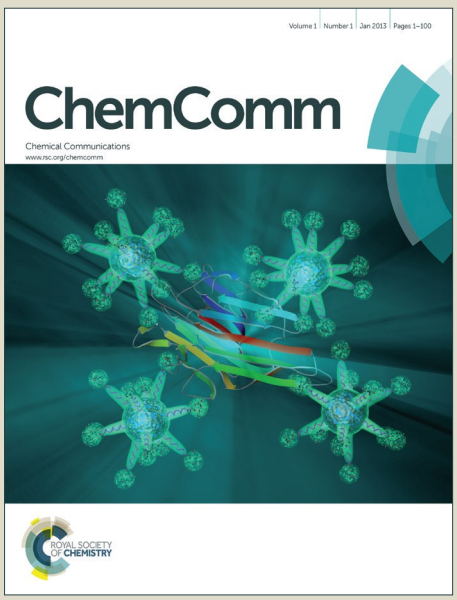

ROYAL SOCIETY OF CHEMISTRY

www.rsc.org/chemcomm

ChemComm

COMMUNICATION

Specific self-monitoring of disassembly of metal-associated amyloid-β aggregates by a fluorescent chelator

Received 00th January 20xx,
Accepted 00th January 20xx

DOI: 10.1039/x0xx00000x

www.rsc.org/

Tao Yang,‡[a] Xiaohui Wang,‡*[ae] Changli Zhang,[b] Xiang Ma,[e] Kun Wang,[e] Yanqing Wang,[c] Jian Luo,[a] Liu Yang,[a] Cheng Yao*[a] and Xiaoyong Wang*[d]

A dual-functional fluorescent chelator can specifically target and disassemble metal-associated Aβ aggregates, and simultaneously self-monitor the disaggregation by fluorescence in brain homogenates of mice with Alzheimer's disease.

Alzheimer's disease (AD), a neurodegenerative disease, is the most common form of dementia affecting over 24 million people worldwide.[1] Amyloid-β (Aβ) plaques, one of the primary pathological hallmarks of AD, would lead to the neuronal dysfunction and cell death in the progression of AD.[2] In this regard, Aβ aggregates have been considered as both biomarkers and therapeutic targets for AD treatment.[3] Although many imaging probes and inhibitors targeting Aβ aggregates have been designed for diagnosis and therapy of AD, none of them are clinical available to date.[4] Very recently, dual-functional probes and inhibitors for Aβ species have been explored for simultaneous drug tracing and AD treatment due to their potential of monitoring the efficacy and safety of drug in real-time.[5] However, the specificity for the target and blood brain barrier (BBB) permeability still need to be improved.

Metal ions, such as zinc and copper with high concentrations in Aβ plaques of AD brains have been shown to promote Aβ aggregation and influence Aβ toxicity, which tightly correlate with AD pathogenesis.[6] Metal chelators have been considered as potential therapeutic agents for AD with the aim of reducing metal-induced Aβ aggregation and neurotoxicity *via* regulating the metal ions distribution.[7] On these bases, modification of chelators with sensing functions would be a promising strategy for developing dual-functional chelators as both probes and inhibitors of metal-induced Aβ aggregation. However, up to now, such chelators capable of specific sensing and disaggregating metal-induced Aβ aggregation are still unknown.

Thioflavin T (ThT), a 2-arylbenzothiazole (ABT) dye is a golden standard probe for amyloid assay to identify the formation of fibrillar aggregates, because it can specifically bind to amyloid fibrils, along with dramatically fluorescence enhancement.[8] Although some drawbacks of ThT limit its application in clinical diagnosis, the perfect affinity of ThT for amyloid fibrils has allowed it served as an excellent starting scaffold for derivatization to develop a number of amyloid probes, which have been used in detection and imaging of amyloid *in vitro* and *in vivo*.[9] Thus, integrating ABT scaffolds into chelating moieties would be feasible to develop fluorescent chelators as both probes and modulators for metal-induced Aβ aggregation. Although a few ABT-based chelators have been reported to selectively bind with Aβ aggregates and modulate the Aβ aggregation,[8] none of them can monitor the disaggregation of metal-induced Aβ aggregates by inherent fluorescence.

To this aim, we herein report a novel fluorescent chelator (TBT) (Fig. 1), as a dual functional probe and disaggregator for Zn^{2+}- and Cu^{2+}-induced Aβ40 aggregation. TBT is composed of a metal-chelating 1,4,7,10-tetraazacyclododecane (cyclen) group and a Aβ-recognizing 2-phenylbenzothiazole group by a linkage strategy. Cyclen was selected for its high modulatory efficacy of metal-induced Aβ aggregation by modification with Aβ binding group.[10] 2-phenylbenzothiazole group as a neutral ABT derivative possesses high lipophilicity and binding affinity to Aβ.[11] Moreover, the fluorescence of 2-phenylbenzothiazole group would be regulated by the coordination of cyclen group with metal ions from Aβ aggregates, because cyclen is a good ligand for photoinduced electron transfer (PET)-based fluorescent sensors.[12] Meanwhile, the aggregates would be disassembled in return (Fig. 1). The synthesis and characterization of TBT are described in ESI† (Scheme S1 and Fig. S1–3). TBT exhibits high affinity for Zn^{2+}– and Cu^{2+}–Aβ

[a] College of Chemistry and Molecular Engineering, Nanjing Tech University, Nanjing 211816, P. R. China. E-mail: wangxhui@njtech.edu.cn; yaocheng@njtech.edu.cn
[b] Department of Chemistry, Nanjing Xiaozhuang College, Nanjing, 210017, P. R. China.
[c] School of Chemistry and Chemical Engineering, Yancheng Teachers University, Yancheng 224002, P. R. China.
[d] State Key Laboratory of Pharmaceutical Biotechnology, School of Life Sciences; State Key Laboratory of Analytical Chemistry for Life Science, Nanjing University, Nanjing, 210093, P. R. China. E-mail: boxwxy@nju.edu.cn
[e] State Key Laboratory of Coordination Chemistry, Nanjing University, Nanjing 210093, P. R. China.
†Electronic Supplementary Information (ESI) available: Experimental details and additional scheme, figures, and tables. See DOI: 10.1039/x0xx00000x
‡Tao Yang and Xiaohui Wang contributed equally.

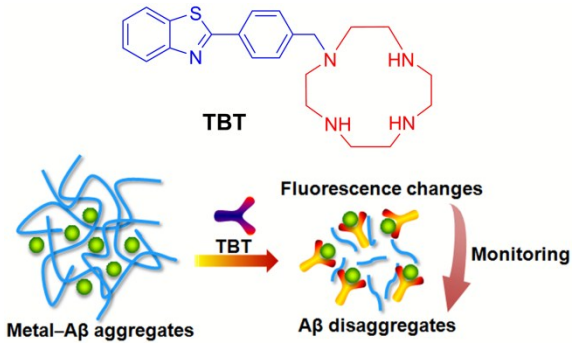

Fig. 1 The structure (top) and design principle (bottom) of TBT.

aggregates over metal-free Aβ aggregates. Most importantly, TBT is able to specifically disaggregate the metal-induced Aβ aggregation and simultaneously monitor *in situ* the disassembly of metal-associated Aβ aggregates by its fluorescence in brain homogenates of AD mice. Surprisingly, TBT can also detoxify the neurotoxicity of metal–Aβ species in living cells and exhibits strong ability to penetrate the BBB of mice. To the best of our knowledge, TBT is the first fluorescent chelator as dual probe and disaggregator for metal-induced Aβ aggregation with high selectivity and BBB permeability.

The binding behaviour of TBT as a chelator for Zn^{2+} or Cu^{2+} was initially investigated by fluorescence titration in buffer, respectively. As expected, TBT can give sensitive fluorescent responses for both Zn^{2+} and Cu^{2+} in 1 : 1 binding mode (Fig. S4, ESI†). Zn^{2+} ions induce fluorescence enhancement of TBT due to the block of PET processes from secondary amines of cyclen to 2-phenylbenzothiazole group upon the reaction of cyclen with Zn^{2+} ions.[13] On the contrary, due to the strong paramagnetic nature of Cu^{2+},[14] a remarkable fluorescence quenching of TBT is observed with addition of Cu^{2+}. Moreover, the association constant (K_a) of TBT with Zn^{2+} and Cu^{2+} was determined to be 4.93×10^6 M^{-1} and 6.8×10^7 M^{-1}, respectively. The results indicate that TBT can tightly bind with Zn^{2+} or Cu^{2+} *via* coordination interactions between cyclen group and the metal ions. Furthermore, TBT also exhibits high selectivity for Cu^{2+} and Zn^{2+} against other relevant biological metal ions (Fig. S5, ESI†).

The binding affinity of TBT for Aβ aggregates was also studied using a ThT fluorescence competition assay. As shown in Fig. 2A, the strong fluorescence of ThT–Aβ system dramatically decrease with the addition of increasing amounts of TBT in the presence of Zn^{2+}, indicating that TBT may displace ThT to bind with Zn^{2+}-associated Aβ40 aggregates, because TBT per se hardly affect the fluorescence of ThT (Fig. S6, ESI†). Moreover, the inhibition constant (K_i) of TBT was calculated to be 1.62 μM, which further reinforced its high affinity for Zn^{2+}–Aβ40 aggregates.[15] On the contrary, the addition of TBT lead to much weaker decrease of the fluorescence of ThT–Aβ system in the absence of Zn^{2+} (inset of Fig. 2A and Fig. S7, ESI†). The results strongly indicate that TBT has much higher binding affinity for Zn^{2+}-induced Aβ40 aggregates than for Zn^{2+}-free Aβ40 aggregates. The capture of cyclen group with Zn^{2+} from the aggregates may promote the binding interactions between 2-phenylbenzothiazole group and Aβ40, consequently boost

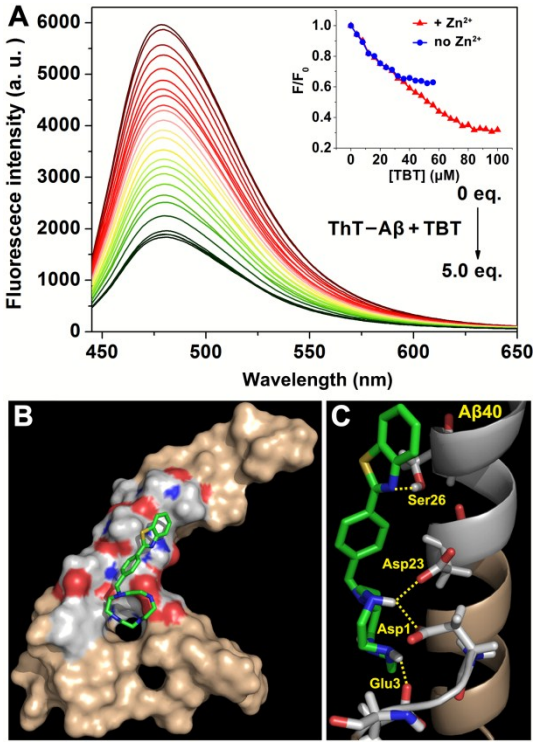

Fig. 2 (A) Fluorescence spectra of ThT (20 μM, λ_{ex} = 415 nm) upon addition of increasing amounts of TBT in the presence of Zn^{2+}-induced Aβ40 fibrils. Inset: the emission intensity ratio (F/F_0) of ThT at 480 nm *versus* the concentration of TBT in the presence Aβ40 fibrils with or without Zn^{2+}. Surface (B) and cartoon (C) representations of TBT interacting with Aβ40 (PDB 1BA4) in energy-minimized average model. Residues Asp23 – Aln30 are depicted in color. The dash lines indicate possible hydrogen bondings.

the binding affinity of TBT for the metal-associated Aβ40 aggregates. To verify the assumption, the affect of cyclen on ThT fluorescence in the presence of Zn^{2+}-induced Aβ40 aggregates was also investigated. The clear decrease of ThT fluorescence implies that cyclen can bind with Zn^{2+} and reduce the degree of aggregates (Fig. S8, ESI†). Thus, a synergistic effect of two function moieties may contribute to the high affinity of TBT with Zn^{2+}–Aβ40 aggregates. Similar results were obtained in the presence of Cu^{2+}–Aβ40 aggregates (Fig. S9, ESI†). Additionally, molecular docking was performed to further understand the binding mode of TBT for Aβ40. The lowest energy docking conformations of TBT–Aβ40 shows that the 2-phenylbenzothiazole group binds preferentially with the central hydrophobic residues (23 – 30 region of Aβ40 peptide), which are also the bind sites for ThT.[16] While cyclen group is close to the binding sites for Zn^{2+} and Cu^{2+} near N-terminal of Aβ40 (Fig. 2B)[17]. Hydrogen bonding between TBT and Ser26, Asp23, Glu3, and Asp1 are probably involved in the association (Fig. 2C). The interaction energies between amino acids of Aβ40 and TBT are listed in Table S1 (ESI†). The results illustrate that TBT is prone to compete with ThT owing to the similar bind sites in Aβ and capture metal ions from metal–Aβ species, which is consistent with the result of ThT fluorescence competition assay.

On the basis of above findings, we next explored the ability of TBT to disaggregate Zn^{2+}- or Cu^{2+}-induced Aβ40 aggregation by *in vitro* experimental approach. The effect of cyclen on

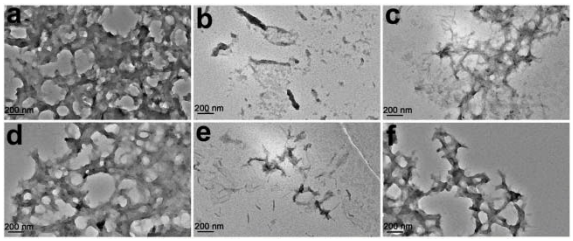

Fig. 3 TEM images of Aβ40 species in disaggregation assay: a, Aβ + Zn^{2+}; b, Aβ + Zn^{2+} + TBT; c, Aβ + Zn^{2+} + cyclen; d, Aβ + Cu^{2+}; e, Aβ + Cu^{2+} + TBT; f, Aβ + Cu^{2+} + cyclen.

disaggregation was also investigated as control. For turbidimetry assay, TBT can cause much lower absorbance intensities at 405 nm of the solution of both Zn^{2+}- and Cu^{2+}-induced Aβ40 aggregates than cyclen (Fig. S10A, ESI†). Using microBCA assay, the amounts of soluble Aβ40 of solution with both Zn^{2+} and Cu^{2+} remarkably increase upon incubation with TBT, which are higher than the situation with cyclen (Fig. S10B, ESI†). Circular dichroism (CD) spectroscopy were further performed to reveal the conversions of secondary structure of Aβ40 among random coil, α-helix, and β-sheet.[18] Upon addition of TBT, the β-sheet structures with a negative band centered at 218 nm disappear, instead, a typical random coil conformation with new positive band at 215 nm is observed (Fig. S11, ESI†).[10a] Moreover, transmission electron microscopy (TEM) visually confirm that TBT can reverse almost all of large amorphous aggregates into only a small amount of short fibrils of Aβ40 (Fig. 3). In constrast, cyclen results in higher amount of small aggregates. Comparatively, TBT can barely reduce the degree of metal-free Aβ aggregation by both turbidimetry and microBCA assays (Fig. S12, ESI†). Interestingly, the fluorescence of TBT also scarcely changes in the presence of metal-free Aβ40 species (Fig. S13, ESI†). These results coherently indicate that TBT can specifically disassemble Zn^{2+}- and Cu^{2+}-induced Aβ40 aggregation over metal-free Aβ40 aggregation. Generally, the selective coordination interactions of cyclen group with Zn^{2+} or Cu^{2+} and high binding affinity of 2-phenylbenzothiazole group with Aβ may cohesively bring out the synergistic effect, which impels TBT to specifically target metal–Aβ aggregates and simultaneously capture the Aβ-associated metal ions to disassemble the aggregates, accompanied with sensitive fluorescence changes. Furthermore, cyclen exhibits much weaker ability to reduce metal-induced Aβ aggregation than that of TBT in the disaggregation assays because of no synergistic effect in it.

Encouraged by the above results, we next tried to monitor the disaggregation of metal–Aβ40 aggregates *via* fluorescence changes of TBT in buffer. Turbidimetry was simultaneously used to evaluate the degree of aggregation. As shown in Fig. 4, the fluorescence intensity of TBT at 375 nm gradually increase upon reaction with performed Zn^{2+}–Aβ aggregates, meanwhile, time-dependent decrease of absorbance intensities at 405 nm are also observed. The capture of TBT with Zn^{2+} from Zn^{2+}–Aβ aggregates not only change its fluorescence, but also simultaneously reduce the degree of Aβ aggregates. Definitely, a correlation between fluorescence intensity of TBT and turbidity may exist according to their synchronous changes

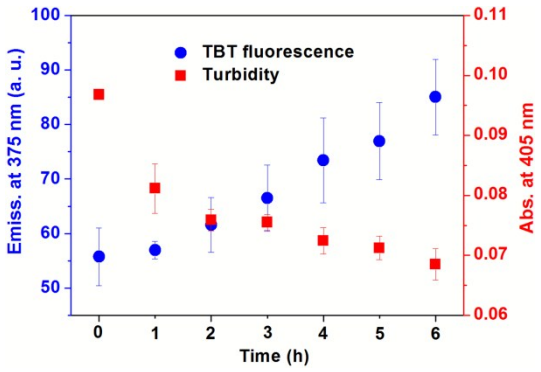

Fig. 4 Fluorescence emission intensity at 375 nm of TBT (20 μM, λ_{ex} = 305 nm) and turbidity (A_{405}) of performed Zn^{2+}–Aβ40 aggregates solution in the presence of TBT after incubation for different periods of time (n = 3).

during the incubation. Therefore, TBT is able to self-monitor the disaggregation of Zn^{2+}–Aβ aggregates caused by itself via fluorescence enhancement without any extraneous labelling agents. Certainly, TBT can also monitor *in situ* the degree changes of Cu^{2+}-induced Aβ aggregation under the same experimental conditions (Fig. S14, ESI†). Moreover, TBT can still exhibit its dual abilities against performed Zn^{2+}–Aβ aggregates under near physiological conditions, such as PBS and HEPES buffer (Fig. S15, ESI†).

In order to test the practical applications of TBT as a dual-functional chelator in a biologically relevant environment, the brain homogenates of APPswe/PSEN1 transgenic mice were used as media because it contains plenty of metal–Aβ aggregates (Fig. 5).[19] Native gel electrophoresis/Western blot analysis was adopted to reveal the reversal effect of TBT on Aβ aggregates from the brain.[10b] As shown in Fig. 5, the incubation with TBT for 24 h result in obvious enhancement of low molecular weight Aβ oligomer species (< 17 KDa) (lanes 2, 4, and 6), compared with control samples (lanes 1, 3, and 5), respectively, implying that TBT is able to reverse Aβ aggregates from the brain of AD mice. Concurrently, the fluorescence intensity of TBT gradually decrease during 24 h incubation, indicating that TBT may target metal–Aβ aggregates and coordinate with Zn^{2+} and Cu^{2+} of the aggregates in AD mice (Fig. S16, ESI†). In terms of the inference, the contents of Zn and Cu of brain homogenates were measured to be *ca*. 15.1 mg/kg and *ca*. 5.1 mg/kg in the brain tissues, respectively, which may be sufficient to induce Aβ aggregation. Moreover, the fluorescence quenching of TBT was observed by varying the $[Zn^{2+}]/[Cu^{2+}]$ ratios due to the stronger quenching effect of Cu^{2+} (Fig. S17, ESI†). Therefore, the decrease of TBT fluorescence in brain homogenates is likely attributed to the coordination with Cu^{2+}. Taken together, TBT is capable of targeting and disaggregating metal-associated Aβ aggregates and self-monitoring the disaggregation by fluorescence decrease even in the brain homogenates of AD mice.

The effect of TBT on metal–Aβ40 neurotoxicity in living cells was also measured using MTT cell viability assays (Fig. S18, ESI†). Treatment of TBT with PC12 cells including Aβ and either Zn^{2+} or Cu^{2+} presents higher cell viability than that of metal–Aβ, suggesting that TBT can detoxify the neurotoxicity of metal-Aβ

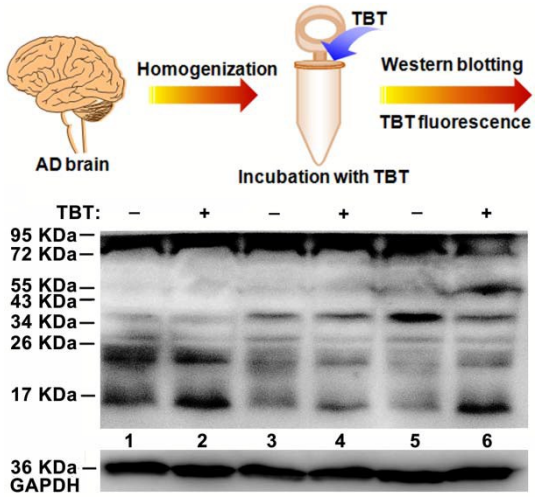

Fig. 5 Top: scheme of disaggregation of TBT in brain homogenates of AD mice. Bottom: Disassembly of TBT against Aβ aggregates from the brain homogenate of APPswe/PSEN1 transgenic mice by native gel electrophoresis using Western blotting with an anti-Aβ antibody 6E10. Lanes 1, 3, and 5 are brain homogenate control of three 6-month-old Tg mice, respectively; Lanes 2, 4, and 6 are homogenates corresponding to the three Tg mice incubated with TBT, respectively. Glyceraldehyde-3-phosphate dehydrogenase (GAPDH) was used as internal reference to ensure equal protein loading.

species. As a contrast, the effect of cyclen is much weaker than that of TBT. Furthermore, considering that TBT fulfills the Lipinski's rules and logBB (Table S2, ESI†),[20] we further tested its BBB penetration using C57BL/6J mice after an i.v. injection. According to HPLC retention time, TBT is observed in brain extraction at 2 min postinjection and reaches its maximum in the brain around 10 min and still maintains its quantities at 30 min after injection. The characteristic peak of TBT almost disappears until 60 min after dosing (Fig. S19, ESI†). Evidently, TBT is able to across BBB efficiently and can be easily washed out. Moreover, fluorescence spectra of TBT in extraction at 10 min postinjection can be seen in Fig. S20 (ESI†), which corroborates the results of HPLC. Shortly, these findings convincingly bolster TBT available *in vivo* studies.

In summary, for the first time, we designed a fluorescent chelator (TBT) as dual-functional probe and disaggregator for specific self-monitoring the disassembly of metal-associated Aβ aggregates by itself *via* fluorescence in brain homogenates of AD mice. Distinctively, TBT is incapable of both sensing and reducing metal-free Aβ aggregation. Considering its specificity, neuroprotectivity, and efficient BBB permeability, TBT may offer a new direction for chelation therapy and significant potential as a theranostic tool for AD. Further optimization of such small-molecular scaffold for fluorescence imaging is in progress in our lab.

We appreciate the financial support from the National Natural Science Foundation of China (Grants: 21301090, 21401106, 21571154, and 21271101), the Natural Science Foundation of Jiangsu Province (Grants: BK20130923, BK20140090, and BK2012671), the Natural Science Foundation of the Jiangsu Higher Education Institutions of China (Grant: 14KJB150011), the Research Fund for Doctoral Program of Higher Education (Grant: 20123221110012), and Jiangsu Government Scholarship for Overseas Studies.

Notes and references

1 L. M. Ittner and J. Götz, *Nat. Rev. Neurosci*., 2011, **12**, 67–72.
2 R. J. Perrin, A. M. Fagan and D. M. Holtzman, *Nature,* 200[illegible], **461**, 916–922.
3 K. Blennow, *Nat. Med*., 2010, **16**, 1218–1222.
4 (a) C. Rodríguez-Rodríguez, M. Telpoukhovskaia and C. Orvi[illegible], *Coord. Chem. Rev*., 2012, **256**, 2308–2332; (b) M. Staderini, M. A. Martín, M. L. Bolognesi and J. C. Menéndez, *Chem. Soc. Rev*., 2015, **44**, 1807–1819.
5 (a) H. Amiri, K. Saeidi, P. Borhani, A. Manafirad and M. Ghavami, *ACS Chem. Neurosci*., 2013, **4**, 1417–1429; (b) X. [illegible] Zhang, Y. L. Tian, P. Yuan, Y. Y. Li, M. A. Yaseen, J. Grutzendler, A. Moore and C. Z. Ran, *Chem. Commun*., 201[illegible], **50**, 11550–11553; (c) L. H. Lu, H. -J. Zhong, M. D. Wang, S. -[illegible] Ho, H. -W. Li, C. -H. Leung and D. -L. Ma, *Sci. Rep-UK.,* 201[illegible], **5:14619**.
6 M. G. Savelieff, A. S. DeToma, J. S. Derrick and M. H. Lim, [illegible] *Chem. Rev*., 2014, **47**, 2475–2482.
7 S. Bolognin, D. Drago, L. Messori and P. Zatta, *Med. Res. Rev*., 2009, **29**, 547–570.
8 S. Noël, S. Cadet, E. Gras and C. Hureau, *Chem. Soc. Rev*., 2013, **42**, 7747–7762.
9 W. E. Klunk, Y. M. Wang, G. -f. Huang, M. L. Debnath, D. [illegible] Holt and C. A. Mathis, *Life Sci*., 2001, **69**, 1471–1484.
10 (a) T. T. Chen, X. Y. Wang, Y. F. He, C. L. Zhang, Z. Y. Wu, [illegible] Liao, J. J. Wang and Z. J. Guo, *Inorg. Chem*., 2009, **48**, 5801–5809; (b) X. H. Wang, X. Y. Wang, C. L. Zhang, Y. Jiao and Z. [illegible] Guo, *Chem. Sci.,* 2012, **3**, 1304–1312.
11 A. A. Reinke and J. E. Gestwicki, *Chem. Biol. Drug Des*., 2011, **77**, 399–411.
12 S. C. Burdette and S. J. Lippard, *Inorg. Chem*., 2002, **41**, 6816–6823.
13 X. H. Wang, T. Yang, J. Luo, L. Yang and C. Yao, *Chem. Commun*., 2015, **51**, 8185–8188.
14 H. S. Jung, P. S. Kwon, J. W. Lee, J. Kim, C. S. Hong, J. W. Kim, S. Yan, J. Y. Lee, J. H. Lee, T. Joo and J. S. Kim, *J. Am. Chem. Soc*., 2009, **131**, 2008–2012.
15 A. Lockhart, L. Ye, D. B. Judd, A. T. Merritt, P. N. Lowe, [illegible] Morgenstern, G. Z. Hong, A. D. Gee and J. Brown, *J. Biol. Chem*., 2005, **280**, 7677–7684.
16 M. Biancalana and S. Koide, *Biochim. Biophys. Acta*., 2010, **1804**, 1405–1412.
17 P. Faller and C. Hureau, *Dalton Trans*., 2009, 1080–1090.
18 C. A. E. Hauser, R. S. Deng, A. Mishra, Y. Loo, U. Khoe, F. [illegible] Zhuang, D. W. Cheong, A. Accardo, M. B. Sullivan, C. Riekel, [illegible] Y. Ying and U. A. Hauser, *Proc. Natl. Acad. Sci. U. S. A.,* 2011, **108**, 1361–1366.
19 E. L. Que, D. W. Domaille and C. J. Chang, *Chem. Rev*., 2008, **108**, 1517–1549.
20 H. van de Waterbeemd and E. Gifford, *Nat. Rev. Drug Discov.*, 2003, **2**, 192–204.

